Trajectory Generation and Control of a Quadrotor with a Cable-Suspended Load – A Differentially-Flat Hybrid System

Koushil Sreenath, Nathan Michael, Vijay Kumar

Abstract— **A quadrotor with a cable-suspended load with eight degrees of freedom and four degrees underactuation is considered and the system is established to be a *differentially-flat hybrid system*. Using the flatness property, a trajectory generation method is presented that enables finding nominal trajectories with various constraints that not only result in minimal load swing if required, but can also cause a large swing in the load for dynamically agile motions. A control design is presented for the system specialized to the planar case, that enables tracking of either the quadrotor attitude, the load attitude or the position of the load. Stability proofs for the controller design and experimental validation of the proposed controller are presented.**

I. Introduction

Cable-suspended systems are underactuated systems, with the control of these systems being extensively studied in the literature. Early work is split into developing controllers for rapid stabilization of the load swing [16], [17], and/or trajectory generation to achieve fast motion of the load with minimal swing [18], [19], [14], [15].

With the introduction of inexpensive micro UAVs and sophisticated sensors in recent years, controllers have been designed to enable these systems to demonstrate aggressive maneuvers [8], dynamic trajectory generation [9], balancing a flying inverted pendulum [4], etc. This leads very well to using UAVs for transportation of external loads. Having grippers for grasping and transporting load is possible, see [10], however the additional inertia of the load results in a slower response for changes in the attitude. An alternative is to have cable-suspended loads, retaining the agility of the aerial vehicle while still achieving the task of lifting and carrying the suspended load.

Transportation of suspended-load systems through UAVs has been studied in recent years. Early attempts involved quasi-static motions to position and orient a suspended load [11]. Control design for the suspended load transportation using single and multiple micro helicopters was studied and demonstrated in [1], [7]. Quadrotors with suspended loads have also been studied, [13], where the quadrotor is flown along a trajectory generated to minimize the load swing at the end of the motion. However, the primary focus in this early research has been to minimize the load swing through a combination of trajectory generation and active feedback control.

An entire class of dynamic motions, where (a) the suspended load is not just restricted to swing minimally, but is rather allowed to undergo large swings while under active
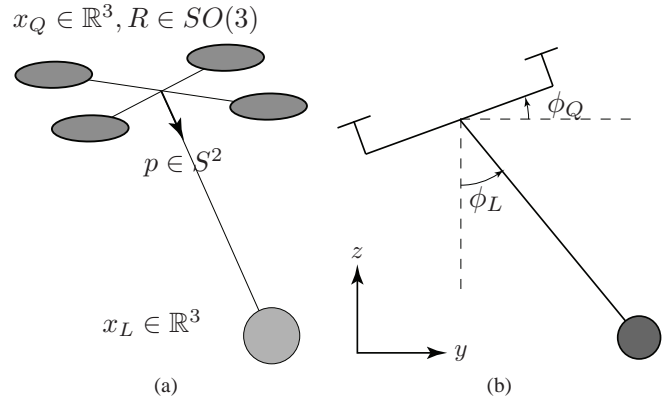
Fig. 1: (a) A 3D quadrotor with a cable suspended load. When the cable is taut, the system evolves on $SE(3) \times S^2$, and has 8 degrees of freedom with 4 degrees of underactuation. (b) A planar quadrotor with a cable suspended load evolving on $SE(2) \times S^1$

feedback control, and (b) the suspended load is allowed to have finite durations of time during which the tension in the cable is zero, have not been addressed. In particular, we wish to study how to control the position of the load, while the load undergoes large swings, and on how to address the case when the tension in the cable goes to zero. More specifically, we would like to design trajectories with phases of large oscillations in the load, and phases when the tension in the cable goes to zero for a finite duration of time, and track the trajectories with appropriately designed feedback controllers.

To demonstrate that such a capability would be necessary, two motivating scenarios are briefly presented next. For instance, to enable a UAV carrying a long cable suspended load to enter / exit short openings (such as a window), the load needs to be dynamically swung into the opening, such that the tension in the cable goes to zero at the right point in time. This enables the UAV to go through the window while the load undergoes free fall, prior to the tension in the cable being reestablished. Alternatively, to enable UAVs to transport suspended loads while flying under a strict ceiling height, either to avoid radar detection or when flying indoors, requires dynamic motion of the load to avoid large obstacles on the ground.

Generating trajectories and designing controllers to enable the load to track these trajectories is hard due to the underactuated nature of the problem, and the switching dynamics that arise when the cable is not taut. This paper studies a quadro-

tor with a cable-suspended load, and develops a coordinate-free dynamic model by employing the Lagrange-d'Alembert principle and considering variations on manifolds. For the quadrotor with the cable suspended load, the dynamics evolve either on $SE(3) \times S^2$, or $SE(3) \times \mathbb{R}^3$, depending on which mode the system is in, i.e., if the cable is taut or not. The quadrotor with cable-suspended load system is shown to be differentially-flat [3], with the position of the load serving as the float output. The notion of a *differentially-flat hybrid system* is introduced, where the dynamics of one flat system switch to the dynamics of another flat system. This enables trajectory generation for the differentially-flat hybrid system, to handle the case when the tension in the cable goes to zero. A controller design is presented for the planar version of the problem, to enable either tracking the quadrotor attitude, the load attitude or the load position. Experimental results are presented to demonstrate the validity of the proposed trajectory generation, and the designed feedback controller.

The paper is organized as follows. Section II develops a coordinate-free dynamical model for the dynamics of a quadrotor with a cable suspended load. Section III demonstrates the differential flatness of the system by presenting a set of flat outputs. The system under consideration is also shown to be a special class of differentially-flat hybrid system. Nominal trajectories are generated and presented. Section IV specializes the developed dynamics to a planar case and develops a three-tier inner-outer loop based control scheme for regulating either the quadrotor attitude, the load attitude or the load position in the plane. Section V presents several experimental results. Finally, Section VI presents concluding remarks.

II. DYNAMIC MODEL OF A QUADROTOR WITH CABLE SUSPENDED LOAD

This section will describe a coordinate-free dynamic model for the quadrotor with a cable suspended load by using rotation matrices for the quadrotor attitude representation and the two-sphere for the load attitude representation. Figure 1a illustrates the system under consideration. We define

$m_Q \in \mathbb{R}$	mass of the quadrotor
$J_Q \in \mathbb{R}^{3 \times 3}$	inertia matrix of the quadrotor with respect to the body-fixed frame
$R \in SO(3)$	rotation matrix of the quadrotor from body-fixed frame to the inertial frame
$\Omega \in \mathbb{R}^3$	angular velocity of the quadrotor in the body-fixed frame
$x_Q, v_Q \in \mathbb{R}^3$	position and velocity vectors of the center of mass of the quadrotor in the inertial frame
$f \in \mathbb{R}$	magnitude of the thrust for the quadrotor
$M \in \mathbb{R}^3$	moment vector for the quadrotor in the body-fixed frame
$m_L \in \mathbb{R}$	mass of the suspened load
$p \in S^2$	unit vector from quadrotor to the load
$\omega \in \mathbb{R}^3$	angular velocity of the suspended load
$x_L, v_L \in \mathbb{R}^3$	position and velocity vectors of the suspended load in the inertial frame.

A. Dynamical Model with Nonzero Cable Tension

The configuration of the system is defined by the location of the load with respect to the inertial frame, the load attitude and the quadrotor attitude. When the cable is taut, the system has eight degrees of freedom with configuration space $Q = SE(3) \times S^2$, and four degree underactuation. The quadrotor and load positions are related by

$$x_Q = x_L - Lp, \tag{1}$$

where L is the cable length, and $p \in S^2$ is the unit vector from quadrotor to the load as defined earlier. The equations of motion are obtained using the method of Lagrange. The Lagrangian for the system, $\mathcal{L} : TQ \to \mathbb{R}$, is defined by $\mathcal{L} = \mathcal{T} - \mathcal{U}$, where $\mathcal{T} : TQ \to \mathbb{R}$ and $\mathcal{U} : Q \to \mathbb{R}$ are the kinetic and potential energies of the mechanism, respectively. These are defined as,

$$T = \frac{1}{2} m_Q v_Q \cdot v_Q + \frac{1}{2} m_L v_L \cdot v_L + \frac{1}{2} \langle \hat{\Omega}, \widehat{J_Q \Omega} \rangle, \tag{2}$$

$$U = m_Q g e_3 \cdot x_Q + m_L g e_3 \cdot x_L, \tag{3}$$

where v_Q is obtained as the derivative of (1), $\langle \cdot, \cdot \rangle : \mathfrak{so}(3) \times \mathfrak{so}(3) \to \mathbb{R}$ is the inner product on $\mathfrak{so}(3)$, and the *hat map* $\hat{\cdot} : \mathbb{R}^3 \to \mathfrak{so}(3)$ is defined such that $\hat{x} y = x \times y, \forall x, y \in \mathbb{R}^3$.

The dynamics of the system satisfy the Lagrange-d'Alembert principle,

$$\delta \int_0^T \left(\mathcal{L} + \langle W_1, \hat{M} \rangle + W_2 \cdot f R e_3 \right) dt = 0, \tag{4}$$

where f is the thrust magnitude, M is the moment vector, and $W_1 = R^T \delta R$, $W_2 = \delta x_Q = \delta x_L - L \delta p$ are variational vector fields [12], with the infinitesimal variations satisfying [6], [2], [5]

$$\delta p = \xi \times p, \ \xi \in \mathbb{R}^3 \text{ s.t. } \xi \cdot p = 0$$
$$\delta \dot{p} = \dot{\xi} \times p + \xi \times \dot{p}$$
$$\delta R = R \hat{\eta}, \ \eta \in \mathbb{R}^3$$
$$\delta \hat{\Omega} = \widehat{\hat{\Omega} \eta} + \dot{\hat{\eta}},$$

with δp being a variation on S^2, and δR a variation on $SO(3)$.

Since (4) is satisfied for all possible variations, the equations of motion for the quadrotor with cable-suspended load are obtained as

$$\dot{x}_L = v_L, \tag{5}$$
$$(m_Q + m_L)(\dot{v}_L + g e_3) = (p \cdot f R e_3 - m_Q L (\dot{p} \cdot \dot{p})) p, \tag{6}$$
$$\dot{p} = \omega \times p, \tag{7}$$
$$m_Q L \dot{\omega} = -p \times f R e_3, \tag{8}$$
$$\dot{R} = R \hat{\Omega}, \tag{9}$$
$$J_Q \dot{\Omega} + \Omega \times J_Q \Omega = M. \tag{10}$$

Remark 1: The quadrotor attitude dynamics in (10) is decoupled from the load attitude and position dynamics in (8), (6) respectively, while the load attitude dynamics is decoupled from the load position dynamics. Also notice that gravity does not influence the load attitude dynamics. Both

these observations will motivate the choice of our control structure in Section IV.

B. Dynamical Model with Zero Cable Tension

When the tension in the cable goes to zero, the system evolves on $Q_z = SE(3) \times \mathbb{R}^3$, with the quadrotor and load as separate systems, with the load being in free fall. The dynamical model in this case is,

$$\dot{x}_L = v_L, \tag{11}$$
$$m_L(\dot{v}_L + ge_3) = 0, \tag{12}$$
$$\dot{x}_Q = v_Q, \tag{13}$$
$$m_Q(\dot{v}_Q + ge_3) = fRe_3, \tag{14}$$
$$\dot{R} = R\hat{\Omega}, \tag{15}$$
$$J_Q\dot{\Omega} + \Omega \times J_Q\Omega = M. \tag{16}$$

Next, for the purpose of the controller design in Section IV, the dynamics (6), (8), (10) are specialized to the planar case.

C. Dynamical Model Specialized to the Plane

The configuration space for the planar quadrotor with cable suspended load is $Q_p := SE(2) \times S^2$, with $q_p := (x_L; \phi_L; \phi_Q) \in Q_p$, where with an abuse of notation, we define $x_L \in \mathbb{R}^2$ as the load position, ϕ_L the roll angle of the load, ϕ_Q the roll angle for the quadrotor; see Figure 1b. Also defining $J_Q \in \mathbb{R}$ the inertia of the quadrotor in the plane, $e_3 = [0,1]^T$, and $p \in S^1, R \in SO(2)$, the dynamics are obtained as,

$$p = \begin{bmatrix} \sin(\phi_L) \\ -\cos(\phi_L) \end{bmatrix}, \quad R = \begin{bmatrix} \cos(\phi_Q) & -\sin(\phi_Q) \\ \sin(\phi_Q) & \cos(\phi_Q) \end{bmatrix}. \tag{17}$$

The dynamical equations of the quadrotor with cable-suspended system specialized to the plane can then be written directly from (6)-(10),

$$(m_Q + m_L)(\dot{v}_L + ge_3) = (f\cos(\phi_Q - \phi_L) - m_Q l\dot{\phi}_L^2)p \tag{18}$$

$$m_Q l\ddot{\phi}_L = \sin(\phi_Q - \phi_L) \tag{19}$$
$$J_Q\ddot{\phi}_Q = M \tag{20}$$

Note that we abused notation and have used the same variable names in both the 3D and the planar case. The controller designed in Section IV will be developed on the planar model presented here.

Next, we demonstrate that the quadrotor with a cable suspended load is differentially flat with the load position being the flat outputs. This holds both in 3D and in the planar case.

III. DIFFERENTIAL FLATNESS

A system is differentially flat if there exists a set of flat outputs, such that the state and inputs of the system can be expressed as smooth functions of the flat outputs and their higher-order derivatives [3]. Differential-flatness has been employed for planning dynamic trajectories for quadrotor systems [9]. Here we demonstrate that the quadrotor with a cable-suspended load is differentially-flat, and moreover it is a differentially-flat hybrid system as defined below.

Definition 1: (Differentially-Flat Hybrid System) Consider the following hybrid system

$$\Sigma : \begin{cases} \dot{x}_1 = f_1(x_1) + g_1(x_1)u_1, & x_1 \notin \mathcal{S}_1 \\ x_2^+ = \Delta_1(x_1^-), & x_1^- \in \mathcal{S}_1 \\ \dot{x}_2 = f_2(x_2) + g_2(x_2)u_2, & x_2 \notin \mathcal{S}_2 \\ x_1^+ = \Delta_2(x_2^-), & x_2^- \in \mathcal{S}_2, \end{cases} \tag{21}$$

and suppose the dynamics of x_1, x_2 are differentially-flat with a set of flat outputs $\mathcal{Y}_1$ and $\mathcal{Y}_2$ respectively, the post-transition value of the outputs $\mathcal{Y}_2$ are a function of the pre-transition value of the flat output $\mathcal{Y}_1$ and its higher-order derivatives, then the system Σ is a differentially-flat hybrid system.

The consequences of having a differentially-flat hybrid system are that everything about the system is encoded in the flat outputs, including the instant when the switching occurs from one dynamics to another. For instance, since the switching surface S_1 is embedded in the state space, and can be written as the zero surface of some function of the state, it can equivalently written as another zero surface of some function of the flat outputs $\mathcal{Y}_1$ and their higher-order derivatives.

To show that the system comprising the quadrotor with a cable-suspended load is differentially-flat, we will look at the dynamical equations of motion arising from Newton-Euler, such that the internal constraint force of the system, corresponding to the tension in the cable, is introduced. Looking at Figure 1a, the equations of motion can be written as,

$$m_Q\ddot{x}_Q = fRe_3 - m_Qge_3 + Tp \tag{22}$$
$$J\dot{\Omega} + \Omega \times J\Omega = M \tag{23}$$
$$m_L\ddot{x}_L = -Tp - m_Lge_3, \tag{24}$$

where $T \in \mathbb{R}$ is the tension in the cable.

Lemma 1: $\mathcal{Y}_1 = (x_L, \psi)$, is a set of flat outputs for the above system, where $\psi \in \mathbb{R}$ is the yaw angle of the quadrotor.

Proof: The quantity Tp can be determined from (24), from which the unit vector $p = Tp/||Tp||$ and the tension $T = Tp \cdot p$ are determined. The quadrotor position can then be determined using (1). All remaining quantities, R, Ω, f, M can be determined from knowledge of x_Q, ψ and their higher-order derivatives, since (x_Q, ψ) are flat outputs for a quadrotor as shown in [9]. ∎

Remark 2: The input M is obtained from the 6th derivative of the position of the load.

Knowing $\mathcal{Y}_1$ and its higher-order derivatives, we know everything about the x_1 system (quadrotor with cable suspended load), including the instant when $x_1^- \in S_1$ and switching would occur. For our system, the transition map Δ_1 maps $x_1^- \in TQ \rightarrow x_2^+ \in TQ_z$. For the x_2 system (quadrotor and free load), knowing $\mathcal{Y}_2 = (x_Q, \psi)$ and its higher order derivatives, and the post-transition state of the load, x_L^+ (which can be computed from $\mathcal{Y}_1$ and its
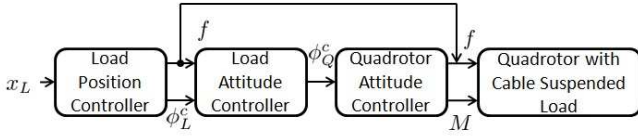
Fig. 2: Controller structure for tracking load position.

derivatives and Δ_1), completely specifies everything about the x_2 system, since the $\mathcal{Y}_2$ is a set of flat outputs for the quadrotor dynamics, and the load dynamics under free fall is analytic and we only require the initial condition x_L^+. Thus, from the flat outputs we can once again determine the pre-transition state, $x2^-$, for the x_2 system and using Δ_2 map this back to the post-transition state x_1^+ for the x_1 system. Thus, the quadrotor with a cable-suspended load is a differentially-flat hybrid system. This fact will be utilized for designing trajectories in Section V.

IV. CONTROL DESIGN

Having derived the dynamics of a general 3-dimensional quadrotor with a cable suspended load system and shown that the load position forms a set of differentially-flat outputs for the system, we will develop a controller that can be used for tracking one of the following quantities (a) quadrotor attitude, (b) load attitude, or (c) load position. Figure 2 illustrates the controller structure. However, the control design will be carried out on the dynamics specialized to the plane. This is done to carry out an initial study and to provide an intuition for designing controllers for the full $3D$ case.

It must be noted that the propositions being presented could be extended to $3D$. For instance [6] develops a quadrotor attitude controller for almost global stabilization on $SO(3)$. Similarly, extending the load attitude controller to 3D should be doable by considering the configuration error function on S^2 defined in [2], but the full load position tracking problem might be hard.

Proposition 1: (*Exponential Stability of Quadrotor Attitude Controlled Flight Mode*) Consider the quadrotor moment defined as

$$M = J_Q(-k_p^Q e_Q - k_d^Q \dot{e}_Q + \ddot{\phi}_Q^d), \quad (25)$$

where $e_Q = \phi_Q - \phi_Q^d$ is the error in tracking the desired quadrotor attitude, and k_p^Q, k_d^Q are positive constants. Then, the quadrotor attitude error dynamics is exponentially stable.

Proof: The quadrotor attitude error dynamics is given by

$$\ddot{e}_Q = \ddot{\phi}_Q - \ddot{\phi}_Q^d = \frac{1}{J_Q}M - \ddot{\phi}_Q^d = -k_p^Q e_Q - k_d^Q \dot{e}_Q, \quad (26)$$

where we substituted for the moment defined in (25). This second order dynamics can be easily shown to be exponentially stable for positive k_p^Q, k_d^Q, and by the converse Lyapunov theorem, there exists a Lyapunov function satisfying

$$z_Q^T M_q z_Q \leq V_Q \leq z_Q^T M_Q z_Q, \quad (27)$$
$$\dot{V}_Q \leq -z_Q^T W_Q z_Q, \quad (28)$$

where $z_Q = [e_Q, \dot{e}_Q]^T \in \mathbb{R}^2$, and $M_q, M_Q, W_Q \in \mathbb{R}^{2\times 2}$ are positive definite matrices. ∎

Proposition 2: (*Exponential Stability of Load Attitude Controlled Flight Mode*) Consider the computed quadrotor attitude defined as

$$\phi_Q^c := \phi_L + \sin^{-1}\left(-k_p^L e_L - k_d^L \dot{e}_L + \frac{\ddot{\phi}_L^d m_Q l}{f}\right), \quad (29)$$

where $e_L = \phi_L - \phi_L^d$ is the error in tracking the desired load attitude, and the initial conditions satisfy

$$|-k_p^L e_L - k_d^L \dot{e}_L + \frac{\ddot{\phi}_L^d m_Q l}{f}| < 1, \quad (30)$$

where $0 < \frac{f}{m_Q l} \leq \alpha$. Define $W_L, W_{LQ} \in \mathbb{R}^{2\times 2}$ as

$$W_L = \begin{bmatrix} \alpha k_p^L c_1 & \frac{\alpha k_d^L c_1}{2} \\ \frac{\alpha k_d^L c_1}{2} & \alpha k_d^L - c_1 \end{bmatrix}, \quad (31)$$

$$W_{LQ} = \begin{bmatrix} c_1 \alpha^2 & \alpha^2 \\ 0 & 0 \end{bmatrix}, \quad (32)$$

where k_p^L, k_d^L, c_1 are positive constants such that,

$$c_1 < \min\{\sqrt{\alpha k_p^L}, \frac{k_p^L k_d^L}{k_p^L + k_d^L/2}\}, \quad (33)$$

$$\lambda_m(W_L) > \frac{||W_{LQ}||^2}{4\lambda_m(W_Q)}, \quad (34)$$

where $\lambda_m(\cdot)$ denotes the minimum eigenvalue of a matrix. Then, the load attitude error dynamics is exponentially stable for all initial conditions satisfying (30).

Proof: See Appendix I. ∎

Proposition 3: (Exponential Stability of Load Position Controlled Flight Mode) Consider the quadrotor thrust and desired load attitude defined as,

$$f = (A + B) \cdot Re_3, \quad (35)$$

$$p_d = -\frac{A}{||A||} \implies \phi_L^d = \tan^{-1}(\frac{-A_1}{A_2}), \quad (36)$$

where A, B are defined as below,

$$A = -k_p^x e_x - k_d^x \dot{e}_x + m_L \ddot{x}_L^d + m_L g e_3 \quad (37)$$
$$B = m_Q \ddot{x}_Q^d + m_Q g e_3$$
$$= m_L \ddot{x}_L^d - m_Q l \ddot{p}^d + m_Q g e_3, \quad (38)$$

and A_1, A_2 are the two components of A. Further assume,

$$||m_L(\ddot{x}_L^d + g e_3) + m_Q(\ddot{x}_Q^d + g e_3)|| \leq C, \quad (39)$$

and assume there exists $d_1, d_2 > 0$, such that,

$$m_Q l||\ddot{p} - \ddot{p}^d|| \leq d_1|e_L| + d_2|\dot{e}_L|. \quad (40)$$

Such a bound exists since p is driven to p^d exponentially. Next, define $W_x \in \mathbb{R}^{2\times 2}, W_1 \in \mathbb{R}^{6\times 6}$ as

$$W_x = \begin{bmatrix} c_2 k_p^x(1+\beta) & \frac{c_2 k_d^x(1+\beta) + k_p^x \beta}{2} \\ \frac{c_2 k_d^x(1+\beta) + k_p^x \beta}{2} & k_d^x(1+\beta) - c_2 \end{bmatrix}, \quad (41)$$

$$W_1 = \begin{bmatrix} 0 & 0 & d_1c_2 + c_2C & d_2c_2 & c_2C & 0 \\ - & 0 & d_1 + C & d_2 & C & 0 \\ - & - & 0 & 0 & 0 & 0 \\ - & - & - & 0 & 0 & 0 \\ - & - & - & - & 0 & 0 \\ - & - & - & - & - & 0 \end{bmatrix}, \quad (42)$$

where the "-" are to be filled to make W_1 symmetric, and k_p^x, k_d^x, c_2 are positive constants such that,

$$c_2 < \min\{\sqrt{k_p^x}, \frac{k_p^x k_d^x (1+\beta)^2}{k_p^x + k_d^{x^2}/4}\}, \quad (43)$$

Then the load position error e_x exponentially goes to zero.

Proof: See Appendix II. ∎

V. EXPERIMENTAL RESULTS

We first discuss trajectory generation prior to presenting results of tracking with the feedback control. We parametrize each flat output as a function of time and pick a suitable basis function. An optimization problem is then posed to solve for the coefficients of the basis polynomials to minimize the sixth-derivative of the load position, subject to constraints of initial and final states. Minimizing the sixth-derivative of the load position ensures minimum snap motion for the quadrotor. Thus we solve,

$$\min \int_{t_0}^{t_1} ||\frac{d^k x_i}{dt^k}||^2 dt, \quad (44)$$

where $x_i(t) = \Sigma_{j=0}^n c_{i,j}\beta_j(t)$, is a parametrized flat output, and $\beta_j(t)$ are the basis functions.

As an example to illustrate the trajectory generation, we choose a sinusoidal basis to generate a trajectory for the load position in 3D. Figure 3 depicts the result of simulating the system dynamics, (6), (8), (10), in open-loop with the feedforward input computed from the differential-flatness. The planned load profile is highlighed, along with the resulting required quadrotor motion to obtain the desired load profile.

With nominal trajectories generated, we study the performance of the proposed controller first in simulation. Figure 4 illustrates tracking of a sinusoidal wave for the load position at close to the natural frequency of the load system. With a cable length of 1m, the load has a natural frequency of $1/2$ Hz. This makes tracking close to this frequency hard. As seen in the figure, even with large initial errors in the load position (upto 1 m in the horizontal load position), the tracking error converges to zero.

Next, we conduct preliminary experiments to demonstrate the validity of the proposed controller. Figure 5 depicts the experimental setup used. A Hummingbird quadrotor is employed along with a suspended load with Vicon markers. The markers enable sensing the load position and the load attitude for use in the feedback control. As a first experiment, we demonstrate tracking of the load position while commanding it to move from one point to another. Figure 6 illustrates the tracking of the load position.
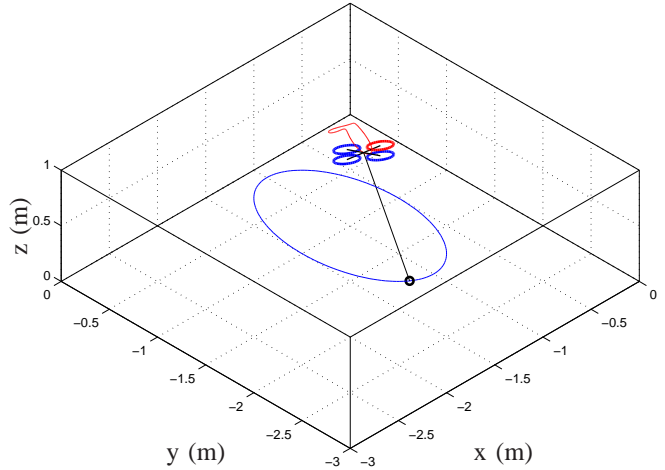

Fig. 3: A nominal trajectory for the load position is generated using the differential-flatness property in 3D. An open-loop simulation is performed with the feedforward moments computed from the flatness. The blue curve shows the planned load trajectory, while the red curve shows the resulting quadrotor motion to obtain the planned load motion.
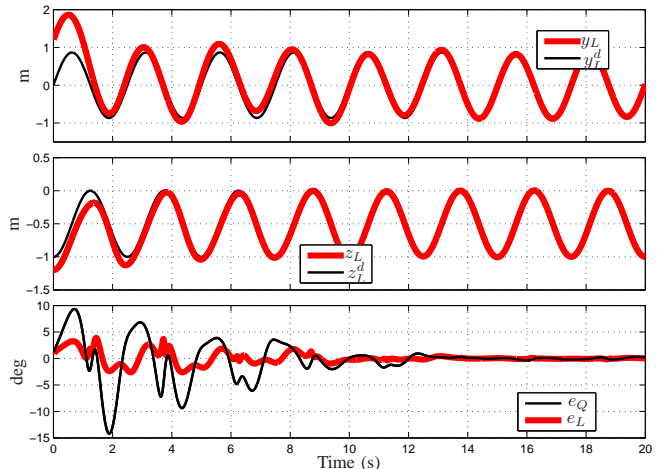

Fig. 4: Simulation results for tracking a sinusoidal load trajectory, close to the natural frequency of the suspended load, with large initial errors. The load and quadrotor trajectories are shown converging to the nominal designed trajectory, and the error in the quadrotor and load attitude converges to zero.

To study the performance of the controller to track the load position while the load is undergoing large oscillations, we design a fixed-amplitude sinusoidal motion for the load in the horizontal and vertical directions. The frequency of motion, however, varies slowly with time, starting at $1/5$ Hz and increasing to the natural frequency of the suspended load at $1/2$ Hz. As expected, controlling the motion of the load while exiting it close to resonance is extremely hard. Our proposed controller is able to track the load trajectory upto a frequency of 0.49 Hz, beyond which the system becomes unstable. Figure 4 illustrates the tracking for this experiment,

Fig. 5: A Hummingbird quadrotor with a cable suspended load. Both the quadrotor and the suspended load are equipped with Vicon markers for enabling sensing their position and attitude for feedback control. The cable length is 1 m, and the load weighs 90 gm.
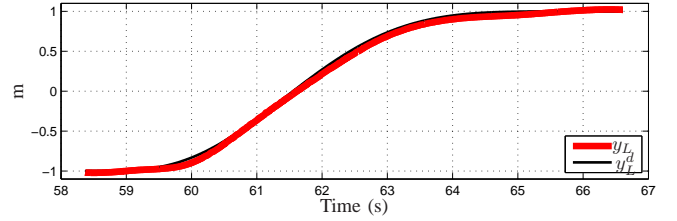

Fig. 6: Experimental results for tracking a trajectory for the load position to move from point-to-point with minimal oscillations in the load.
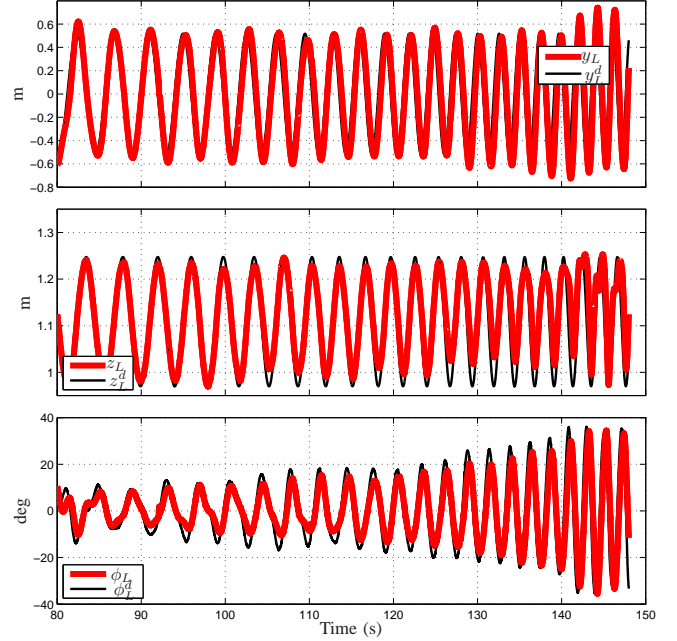

Fig. 7: Experimental results for tracking a fixed-amplitude sinusoidal load trajectory for both the horizontal and vertical positions of the load. The frequency of the sinusoid varies slowly from $1/5$ Hz to very close to the natural frequency of the suspended load ($1/2$ Hz. Plots of the horizontal, and vertical load positions along with the load angle is shown. The proposed controller tracks the load position until 0.49 Hz, during when the load is swinging almost 40 deg.

with plots for the horizontal and vertical position tracking of the load, and the load angle. As can be seen, the load has to swing almost 40 deg at the very end to track the load position. The constant offset in tracking the vertical position of the load is due to not correcting for the small variations that occur in the system mass (different batteries weigh different) and in the thrust to rotor speed mapping that changes with temperature and other environmental conditions. Figure 8 shows the tracking in the plane. Correcting for the constant offset in the vertical tracking would result in a better aligned plot. Figure 9 illustrates the horizontal motion of the quadrotor to achieve tracking of the load position. Notice the reduction of peak-to-peak motion of the quadrotor by almost 70% at the end of the trajectory. To track a faster frequency load trajectory, the quadrotor moves less, while the load swings more.

This shows fairly good tracking of the load position even for large oscillations of the load at frequencies close to the natural frequency of the suspended load, validating the controller design. It must be noted that additional experiments for performing load tracking, where the tension in the cable goes to zero for a part of the trajectory will need to be done for a complete experimental validation of the proposed method.

VI. CONCLUSION

We have presented a coordinate-free development of the dynamics of a quadrotor with a cable suspended load, and have shown that this system is a differentially-flat hybrid system. An inner-outer loop-based controller has been de-

signed for the planar case. The flatness property has been utilized to design trajectories and preliminary results have been demonstrated in simulations and in experiments.

This work provides several future paths. Firstly, the presented controller will be studied to extend it to the full 3D case. Early investigations demonstrate that the load attitude can be almost globally stabilized on S^2. Another path to take is to study cooperative, dynamic manipulation of a suspended load, which is more interesting and challenging due to the high degree of freedom. For instance, for planar two quadrotor system with a shared cable suspended load, a system with seven degrees of freedom and three degrees of underaction, the system can be shown to be differentially-flat with four flat outputs.
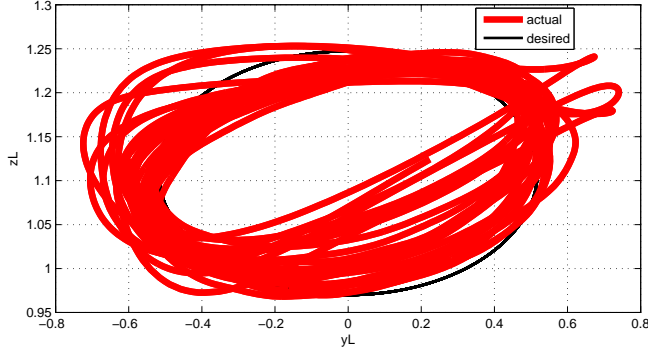
Fig. 8: Experimental results for tracking a fixed-amplitude sinusoidal load trajectory with varying frequency. Correcting for the constant offset in tracking the vertical position of the load could potentially result in a better alignment with the nominal trajecotry.
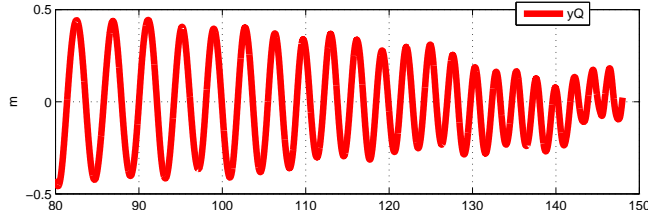

Fig. 9: Experimenally obtained horizontal motion of the quadrotor to track the fixed-amplitude sinusoidal load trajectory with varying frequency. Notice the peak-to-peak reduction in the quadrotor motion by almost 70% to enable tracking the load position. At larger frequencies, the quadrotor moves less, while the load swings more. Vertical quadrotor motion does not change significantly and is not shown.

APPENDIX I
PROOF OF PROPOSITION 2

The load attitude error dynamics is given by

$$
\begin{aligned}
\ddot{e}_L &= \ddot{\phi}_L - \ddot{\phi}_L^d = \frac{\sin(\phi_Q - \phi_L)}{m_Q l} f - \ddot{\phi}_L^d \\
&= \frac{\sin(\phi_Q^d - \phi_L)}{m_Q l} f - \ddot{\phi}_L^d + X, \qquad (45)
\end{aligned}
$$

where $X \in \mathbb{R}$ is defined as,

$$
\begin{aligned}
X &= \frac{\sin(\phi_Q - \phi_L) - \sin(\phi_Q^d - \phi_L)}{m_Q l} f \\
&= \frac{2\sin(\frac{e_Q}{2})\cos(\frac{\phi_Q + \phi_Q^d - 2\phi_L}{2})}{m_Q l} f. \qquad (46)
\end{aligned}
$$

Substituting for ϕ_Q^d in (45) with ϕ_Q^c defined in (29), we obtain,

$$
\ddot{e}_L = \frac{f}{m_Q l}(-k_p^L e_L - k_d^L \dot{e}_L) + X. \qquad (47)
$$

Consider a candidate Lyapunov function given by,

$$
V_L = \frac{\alpha k_p^L}{2} e_L^2 + \frac{1}{2}\dot{e}_L^2 + c_1 e_L \dot{e}_L. \qquad (48)
$$

The time derivative of V_1 along trajectories of the system is given by,

$$
\begin{aligned}
\dot{V}_L &= \alpha k_p^L e_L \dot{e}_L + \dot{e}_L \ddot{e}_L + c_1 \dot{e}_L^2 + c_1 e_L \ddot{e}_L \\
&\leq \alpha(\dot{e}_L + c_1 e_L)(-k_p^L e_L - k_d^L \dot{e}_L + X) + \alpha k_p^L e_L \dot{e}_L + c_1 \dot{e}_L^2 \\
&= -\alpha k_p^L c_1 e_L^2 - (\alpha k_d^L - c_1)\dot{e}_L^2 - \alpha k_d^L c_1 e_L \dot{e}_L + \\
&\quad \alpha(\dot{e}_L + c_1 e_L)X.
\end{aligned}
$$
$$(49)$$

Next we obtain a bound on X in (46) by making a small angle assumption on e_Q and using the fact that the cosine term in (46) is upper bounded by 1, to obtain

$$
X \leq \frac{f}{m_Q l} e_Q \leq \alpha \, e_Q,
$$

where α is as defined in the Proposition. Substituting this into (49), we obtain,

$$
\dot{V}_L \leq -z_L^T W_L z_L + (\dot{e}_L + c_1 e_L)\alpha^2 \, e_Q, \qquad (50)
$$

where $z_L = [e_L, \dot{e}_L]^T \in \mathbb{R}^2$ and W_L as defined in (31).

The condition on c_1 in (33) ensures positive-definiteness of the matrices W_L and $M_l, M_L \in \mathbb{R}^{2\times2}$ where,

$$
M_l = \frac{1}{2}\begin{bmatrix} \alpha k_p^L & -c_1 \\ -c_1 & 1 \end{bmatrix}, \quad M_L = \frac{1}{2}\begin{bmatrix} \alpha k_p^L & c_1 \\ c_1 & 1 \end{bmatrix}, \qquad (51)
$$

such that a bound on the Lyapunov function V_L can be written as

$$
z_L^T M_l z_L \leq V_L \leq z_L^T M_L z_L.
$$

Taking the Lyapunov function $V_{LQ} = V_L + V_Q$ for the subsystem comprising the load and quadrotor attitude dynamics, we have a bound on V_{LQ} as,

$$
z_L^T M_l z_L + z_Q^T M_q z_Q \leq V_{LQ} \leq z_Q^T M_Q z_Q + z_L^T M_L z_L. \quad (52)
$$

Moreover, the time-derivative of V_{LQ} is given by,

$$
\dot{V}_{LQ} \leq -z_L^T W_L z_L + z_L^T W_{LQ} z_Q + -z_Q^T W_Q z_Q, \qquad (53)
$$

where W_{LQ} is as defined in (32).

From the assumptions of Proposition 1, and the conditions on c_1, we have all the following matrices $M_q, M_Q, W_Q, M_l, M_L, W_L$ and the Lyapunov function V_{LQ} to be positive-definite, and

$$
\begin{aligned}
\dot{V}_{LQ} \leq &-\lambda_m(W_L)\|z_L\|^2 + \|W_{LQ}\|_2\|z_L\|\|z_Q\| \\
&- \lambda_m(W_Q)\|z_Q\|^2
\end{aligned}
$$
$$(54)$$

The condition given by (34) ensures $\dot{V}_{LQ}$ becomes negative-definite. Therefore the load and quadrotor attitude error dynamics exponentially converge to zero.

APPENDIX II
PROOF OF PROPOSITION 3

Instead of looking at the load position dynamics (6) or its planar analogue (18), we form a simpler equation by looking at the dynamics of x_{com}, the center of mass of the system. We have,

$$
\begin{aligned}
(m_Q + m_L)\ddot{x}_{com} &= m_Q \ddot{x}_Q + m_L \ddot{x}_L \\
&= fRe_3 - (m_Q + m_L)ge_3, \quad (55)
\end{aligned}
$$

which yields,

$$(m_Q + m_L)\ddot{x}_L = -(m_Q + m_L)ge_3 + m_Q l\ddot{p} + fRe_3, \quad (56)$$

where we have differentiated (1) twice with respect to time and used in the above equation. Defining the load position error as $e_x = x_L - x_L{}^d, e_v = \dot{e}_x$, the error dynamics are given by,

$$
\begin{aligned}
(m_Q + m_L)\dot{e}_v &= -(m_Q + m_L)ge_3 + m_Q l\ddot{p} + \\
&\quad fRe_3 - (m_Q + m_L)\ddot{x}_L^d \\
&= -k_p^x e_x - k_d^x \dot{e}_x + m_Q l(\ddot{p} - \ddot{p}_d) + Y,
\end{aligned}
$$

where $Y \in \mathbb{R}$ is defined as,

$$
\begin{aligned}
Y &= fRe_3 - B - \frac{f - B \cdot Re_3}{p_d \cdot Re_3} p_d \\
&= \frac{f\left((p_d \cdot Re_3)Re_3 - p_d\right) + (B \cdot Re_3)p_d - (p_d \cdot Re_3)B}{p_d \cdot Re_3},
\end{aligned}
$$

such that,

$$
\begin{aligned}
||Y|| &\leq |e_L + e_Q|(||A + B|| + ||B||) \\
&\leq |e_L + e_Q|(k_p^x||e_x|| + k_d^x||\dot{e}_x|| + C), \quad (57)
\end{aligned}
$$

where C is as defined in (39), and $0 < 1/|p_d \cdot Re_3| \leq |e_L + e_Q| \leq \beta \leq 1$.

Consider a candidate Lyapunov function given by,

$$V_x = \frac{k_p^x}{2}e_x \cdot e_x + \frac{1}{2}e_v \cdot e_v + c_2 e_x \cdot e_v. \quad (58)$$

The time derivative of V_x along trajectories of the system is given by,

$$
\begin{aligned}
\dot{V}_x =&\, k_p^x e_x \cdot e_v + c_2 e_v \cdot e_v + (e_v + c_2 e_x) \cdot \dot{e}_v \\
\leq&\, -(k_d^x - c_2)e_v \cdot e_v - c_2 k_p^x e_x \cdot e_x - c_2 k_d^x e_x \cdot e_v + \\
&\, (e_v + c_2 e_x)(d_1|e_L| + d_2|\dot{e}_L| + Y) \\
\leq&\, -(k_d^x - c_2)||e_v||^2 - c_2 k_p^x ||e_x||^2 - c_2 k_d^x ||e_x||||e_v|| + \\
&\, d_1(e_v + c_2 e_x)|e_L| + d_2(e_v + c_2 e_x)|\dot{e}_L| \\
&\, (e_v + c_2 e_x)|e_L + e_Q|(k_p^x||e_x|| + k_d^x||\dot{e}_x|| + C)) \\
\leq&\, -z_x^T W_X z_x + z^T W_1 z,
\end{aligned}
$$
$$(59)$$

where, $z_x = [||e_x||, ||e_v||], z = [z_x, z_L, z_Q]$, and W_X, W_1 are as defined in (41),(42). The condition on c_2 in (43) ensures positive-definiteness of the matrices W_X and $M_x, M_X \in \mathbb{R}^{2\times 2}$ are defined similar to (51), such that a bound on the Lyapunov function V_x can be written as

$$z_x^T M_x z_x \leq V_X \leq z_x^T M_X z_x.$$

Next, considering the Lyapunov function $V = V_x + V_{LQ}$ for the complete system, we can perform a similar analysis to demonstrate exponential stability of the load error dynamics. We have a bound on V as,

$$z^T M_1 z \leq V \leq z^T M_2 z,$$

where $M_1 = diag[M_x, M_l, M_q]$, and $M_2 = diag[M_X, M_L, M_Q]$. Moreover, the time-derivative of V is given by,

$$\dot{V} \leq -z^T W z + z^T(W_1 + W_{LQ})z,$$

where $W = diag[W_X, W_L, W_Q]$.

REFERENCES

[1] M. Bernard and K. Kondak, "Generic slung load transportation system using small size helicopters," *2009 IEEE International Conference on Robotics and Automation*, pp. 3258–3264, May 2009.

[2] F. Bullo and A. D. Lewis, *Geometric Control of Mechanical Systems*. New York-Heidelberg-Berlin: Springer-Verlag, 2004.

[3] M. Fliess, J. Lévine, P. Martin, and P. Rouchon, "Flatness and defect of non-linear systems: introductory theory and examples," *International journal of control*, vol. 61, pp. 1327–1361, 1995.

[4] M. Hehn and R. D'Andrea, "A flying inverted pendulum," *2011 IEEE International Conference on Robotics and Automation*, no. 2, pp. 763–770, May 2011.

[5] T. Lee, M. Leok, and N. H. McClamroch, "Discrete Control Systems," *Springer Encyclopedia of Complexity and Systems Science*, pp. 2002—-2019, 2008.

[6] T. Lee, M. Leok, and N. H. Mcclamroch, "Geometric Tracking Control of a Quadrotor UAV on SE (3)," in *IEEE Conference on Decision and Control*, no. 3, Atlanta, GA, 2010, pp. 5420–5425.

[7] I. Maza, K. Kondak, M. Bernard, and A. Ollero, "Multi-UAV Cooperation and Control for Load Transportation and Deployment," *Journal of Intelligent and Robotic Systems*, vol. 57, no. 1-4, pp. 417–449, Aug. 2010.

[8] D. Mellinger, N. Michael, and V. Kumar, "Trajectory generation and control for precise aggressive maneuvers with quadrotors," *The International Journal of Robotics Research*, vol. 31, no. 5, pp. 664–674, Jan. 2012.

[9] D. Mellinger and V. Kumar, "Minimum snap trajectory generation and control for quadrotors," *2011 IEEE International Conference on Robotics and Automation*, pp. 2520–2525, May 2011.

[10] D. Mellinger, Q. Lindsey, M. Shomin, and V. Kumar, "Design, modeling, estimation and control for aerial grasping and manipulation," *2011 IEEE/RSJ International Conference on Intelligent Robots and Systems*, pp. 2668–2673, Sep. 2011.

[11] N. Michael, J. Fink, and V. Kumar, "Cooperative manipulation and transportation with aerial robots," *Autonomous Robots*, vol. 30, no. 1, pp. 73–86, Sep. 2010.

[12] J. Milnor, *Morse Theory*. Princeton: Princeton University Press, 1963.

[13] I. Palunko, R. Fierro, and P. Cruz, "Trajectory generation for swing-free maneuvers of a quadrotor with suspended payload: A dynamic programming approach," *2012 IEEE International Conference on Robotics and Automation*, pp. 2691–2697, May 2012.

[14] J. Schultz and T. Murphey, "Trajectory generation for underactuated control of a suspended mass," *2012 IEEE International Conference on Robotics and Automation*, pp. 123–129, May 2012.

[15] G. Starr, J. Wood, and R. Lumia, "Rapid Transport of Suspended Payloads," in *International Conference on Robotics and Automation*, no. April, 2005, pp. 1394–1399.

[16] N. Yanai, M. Yamamoto, and A. Mohri, "Feedback Control for Wire-Suspended Mechanism with Exact Linearization," in *International Conference on Intelligent Robots and Systems*, no. October, 2002, pp. 2213–2218.

[17] J. Yu, F. L. Lewis, and T. Huang, "Nonlinear Feedback Control of a Gantry Crane," no. June, 1995.

[18] D. Zameroski, G. Starr, J. Wood, and R. Lumia, "Rapid Swing-Free Transport of Nonlinear Payloads Using Dynamic Programming," *Journal of Dynamic Systems, Measurement, and Control*, vol. 130, no. 4, p. 041001, 2008.

[19] D. Zameroski, G. Starr, J. Wood, R. Lumia, and A. P. Work, "Swing-Free Trajectory Generation for Dual Cooperative Manipulators using Dynamic Programming," in *International Conference on Robotics and Automation*, no. May, 2006, pp. 1997–2003.